

1 **Impact of LUCC on Streamflow Based on the SWAT Model over the**
2 **Wei River Basin on the Loess Plateau of China**

3

4 Hong Wang, Fubao Sun*

5 Key Laboratory of Water Cycle and Related Land Surface Processes, Institute of
6 Geographic Science and Natural Resources Research, Chinese Academy of Sciences,
7 Beijing 100101, China.

8 *Corresponding author: Fubao Sun (sunfb@igsnrr.ac.cn)

9

10

11

12

13

14

15

16

17

18

19

20

21

22

23 **Abstract:** Under the Grain for Green project in China, vegetation recovery constructions have
24 been widely implemented on the Loess Plateau for the purpose of soil and water conservation.
25 Now it becomes controversial whether the recovery constructions of vegetation, particularly forest,
26 is reducing streamflow in rivers of the Yellow River Basin. In this study, we choose the Wei River,
27 the largest branch of the Yellow River and implemented with revegetation constructions, as the
28 study area. To do that, we apply the widely used Soil and Water Assessment Tool (SWAT) model
29 for the upper and middle reaches of the - Wei River basin. The SWAT model was forced with daily
30 observed meteorological forcings (1960-2009), calibrated against daily streamflow for 1960-1969,
31 validated for the period of 1970-1979 and used for analysis for 1980-2009. To investigate the
32 impact of the LUCC (Land Use and land Cover Change) on the streamflow, we firstly use two
33 observed land use maps of 1980 and 2005 that are based on national land survey statistics emerged
34 with satellite observations. We found that the mean streamflow generated by using the 2005 land
35 use map decreased in comparison with that using the 1980 one, with the same meteorological
36 forcings. Of particular interest here, we found the streamflow decreased in agricultural land but
37 increased in forest area. More specifically, the surface runoff, soil flow and baseflow all decreased
38 in agricultural land, while the soil flow and baseflow of forest were increased. To investigate that,
39 we then designed five scenarios including (S1) the present land use (1980), (S2) 10%, (S3) 20%,
40 (S4) 40% and (S5) 100% of agricultural land was converted into mixed forest. We found that the
41 streamflow consistently increased with agricultural land converted into forest by about 7.4 mm per
42 10%. Our modeling results suggest that forest recovery constructions have positive impact on both
43 soil flow and base flow compensating reduced surface runoff, which leads to a slight increase in
44 streamflow in the Wei River with mixed landscapes of Loess Plateau and earth-rock mountain.

45 **1. Introduction**

46 Since 1999, China's Grain for Green project has greatly increased the vegetation cover
47 (Chen et al., 2015) and the total conversion area reaches 29.9 million ha until 2014 (Li, 2015).
48 And the proposals are to further return another 2.83 million ha farmland to forest and grassland by
49 2020 (NDRC, 2014). The establishment of either forest or grassland on degraded cropland has
50 been proposed as an effective approach to mitigating climate change because these types of land
51 use can increase soil carbon stocks (Yan et al., 2012; Deng et al., 2013). Implementation of large
52 scale Grain for Green project is undoubtedly one type of geoengineering which not only mitigates
53 climate change but also is expected to alter hydrological cycle (Lacombe et al., 2016; Lacombe et
54 al., 2008).

55 Some researchers have urged a cessation on Grain for Green expansion on the Loess Plateau
56 of China and argued that continued expansion of revegetation would cause more harm than good
57 to communities and the environment (Chen et al., 2015). One important reason was that the Grain
58 for Green project lead to annual streamflow of the Yellow River declining (Chen et al., 2015; Li,
59 2001). Land use change can disrupt the surface water balance and the partitioning of precipitation
60 into evapotranspiration, runoff, and groundwater flow (Sriwongsitanon and Taesombat, 2011;
61 Foley et al., 2005; Wagner et al., 2013). Large scale revegetation constructions change hydrologic
62 cycle process and distribution of water resources. There are three controversial points of view
63 about the impact of vegetation on streamflow as a whole. Quite a few catchment studies indicated
64 that annual streamflow decreased with revegetation increasing (Zhang and Hiscock, 2010; Bosch
65 and Hewlett, 1982; VanShaar et al., 2002; Mango et al., 2011; Farley et al., 2005; Liu and Zhong,
66 1978) or increased with vegetation destruction (Bosch and Hewlett, 1982; Woodward et al., 2014;

67 Hibbert, 2001), where some catchment studies indicated baseflow of forests was lower due to their
68 high evapotranspiration rates (Lørup et al., 1998; Lorup and Hansen, 1997; Smith and Scott, 1992),
69 while other studies indicated the baseflow increased in the dry season due to higher infiltration
70 and recharge of subsurface storage (the “sponge-effect hypothesis”) (Price, 2011; Lørup et al.,
71 1998; Ogden et al., 2013). In contrast, other studies showed that vegetation has a positive impact
72 on streamflow (Tobella et al., 2014; Li et al., 2001) or no impact on streamflow (Wang, 2000;
73 Beck et al., 2013).

74 To interpret the controversial results, it was argued that the impact of vegetation on annual
75 streamflow depends on watershed area and the relationship between them was negative in smaller
76 watershed and positive in larger watershed (Huang et al., 2009; Zhang, 1984). Some of them
77 thought it was probably the large amount of transpiration water played the main function in
78 hydrological process when the watershed was smaller. And some thought that the different impacts
79 of area probably because the forest of larger watershed could increase precipitation and vegetation
80 was also conducive for the infiltration of precipitation, which increased the proportion of the
81 underground flow of streamflow in forest region. Some researchers indicated tree planting has
82 both negative and positive effects on water resources and the overall effect was the result of a
83 balance between them, which were strongly dependant on tree density (Tobella et al., 2014).
84 Lacombe et al. (2016) found soil infiltrability was an important factor for explaining two modes of
85 afforestation (natural regeneration vs. planting) led to opposite changes in streamflow regime.
86 Huang (1982) analyzed Soviet research results found that 48% runoff coefficients increased, 32%
87 has no change, and 20% decreased with watershed forest increasing. The increased regions were
88 located at high latitude and humid areas. Under this condition, the total evaporation in wooded

89 areas and woodless area are equal. The speculation was that snow may be blown away or to
90 wooded areas from woodless area, which could enhance the coefficient of streamflow but these
91 factors would be weaker over low to middle latitude than that in high latitude (Huang, 1982).
92 Further, vegetation may change hydrological cycle as follows (Le Maitre et al., 1999): redirection
93 of precipitation by the canopy; branches, stem and litter tends to intercept more water into the soil;
94 roots may provide channels for the flow infiltrating to groundwater and extract soil water as
95 evaporation. Hence different results have led to contentious relationship between vegetation and
96 streamflow (Bradshaw et al., 2007; Dijk et al., 2009).

97 The Wei River is one main branch of the Yellow River and has been widely implemented
98 measures of soil and water conservation since the 1980s (Fig. 1). Meanwhile the annual
99 streamflow of the Wei River has decreased significantly since the 1980s (Liu and Hu, 2006; Lin
100 and Li, 2010; Wang et al., 2011). Since the 1990s, the streamflow has sharply dropped and the
101 observed streamflow of Linjiacun station in the 1990s was less than one third of that before 1990s.
102 The terrace and check dam both had a negative effect on annual streamflow which was a result of
103 the balance between the streamflow reducing in the flood season and baseflow increasing in
104 non-flood season on the Loess Plateau (Shao et al., 2013a; Xu et al., 2013). But the impacts of
105 vegetation on streamflow are controversial and complicated. Meanwhile on the Loess Plateau, it
106 was found that there is a drying layer of soil underneath forest with a depth of over 1 m to 3 m
107 from the soil surface owing to serious soil desiccation in water-limited ecosystems (Li, 2001;
108 Wang, 2010a). The land use, rainfall, soil type and slope gradient had a significant impact on dried
109 soil layer thickness (Wang, 2010b). And the great water deficit prevents gravitational infiltration
110 of rainfall and replenishment of groundwater. So forests on the Loess Plateau reduced streamflow

111 as the results of increased retention of rainfall and reduced recharge into ground water (Li, 2001;
112 Tian, 2010). But for earth-rock mountain landscape, vegetation grows on thinner soil layer of rock
113 mountain, which is apt to be saturated and produce soil flow on relatively impermeable rock. So
114 the streamflow in wooded areas might be larger than that in adjacent woodless areas. Under this
115 situation, forests may have positive impact for producing streamflow (Liu and Zhong, 1978).

116 To investigate that, we develop hydrological experiments based on the widely used SWAT
117 model and observed hydrological/ meteorological data and land use data in the Wei River. We aim
118 at understanding possible impact of revegetation constructions, especially the forest restoration on
119 streamflow and its components in the Wei River, which is not only the largest branch of the
120 Yellow river but also with very mixed landscape with the loess plateau and earth-rock mountain.
121 In Sect. 2, we describe the study area and data. In Sect. 3, we set up, calibrate, and validate the
122 SWAT model in the Wei River. Section 4 reports the numerical experiment results, which is then
123 followed by the conclusion in Sect. 5.

124 **2. Study area and data**

125 **2.1 Study area**

126 Wei River is the largest tributary of the Yellow River, which originates from the north of the
127 Wushu mountain at an altitude of 3495 m (involving Gansu, Ningxia and Shaanxi Provinces), and
128 runs across 818 km through into the Yellow River at Tongguan County, Shaanxi Province. In this
129 study, we choose the basin of the upper and middle reaches ($4.68 \times 10^4 \text{ km}^2$) of the Wei River basin
130 ($103.97^\circ \sim 108.75^\circ \text{ E}$, $33.69^\circ \sim 36.20^\circ \text{ N}$, $13.48 \times 10^4 \text{ km}^2$). And the Linjiacun, Weijiabu and
131 Xianyang hydrological stations are used from upstream to midstream in this study (Fig. 2), which
132 divided the study area into 3 regions. Linjiacun station locates at the control section of the

133 upstream and Xianyang station is the control station of middle reaches.

134 Geologically, the basin consists of the Loess Plateau and Qinling Mountain in the respective
135 north and south of the Wei River (Fig. 2). In the north, there are fewer tributaries, whose lengths
136 are further and the gradient is smaller. While in the south, abundant tributaries originate from
137 Qinling Mountain which is steep and close to the river. So the tributaries are shorter and the flows
138 are swifter. And there distribute lots of earth-rock mountain landscape and gravel riverbed in the
139 piedmont.

140 **2.2 Land Use and land Cover Change (LUCC) data**

141 We obtained observed LUCC data from National Science & Technology Infrastructure of
142 China, National Earth System Science Data Sharing Infrastructure (Fig. 3)
143 (<http://www.geodata.cn>). Land use maps for the years of 1980 and 2005 were interpreted based on
144 the corresponding national land use survey data (1:100,000), satellite image, the MODIS data,
145 250-meter space resolution data and combined with pasture resources map (1:500,000), soil type
146 map (1:1,000,000), vegetation type map (1:1,000,000) and other auxiliary data. The LUCC data
147 were divided into six types and further 25 subtypes. And the six types included forest, shrubland,
148 pasture, cropland, water bodies and residential areas: ① The forest type includes Range-Brush
149 (RNGB), Forest-Mixed (FRST), Forest-Deciduous (FRSD), Pine (PINE) and Forest-Evergreen
150 (FRSE); ② The pasture type includes Pasture (PAST), Winter Pasture (WPAS) and
151 Range-Grasses (RNGE); ③ The cropland means Agricultural Land (AGRL); ④ Water includes
152 water (WATR) and Wetlands-Mixed (WETL); ⑤ The residential areas include area of
153 Residential-High Density (URHD) and Residential-Medium Density (URMD); ⑥ The code of
154 bare type is BARE. The area of agricultural land decreased about 7.26% and forest area increased

155 0.81% in 2005 compared with 1980 for the study area.

156 **2.3 Soil data**

157 Soil data were obtained from National Science & Technology Infrastructure of China,
158 National Earth System Science Data Sharing Infrastructure (Fig. 4(a)) (<http://www.geodata.cn>).
159 This soil data map reflects the distribution and characteristics of different soil type and digitized
160 based on 1:500,000 remote sensing digital figures of environment on Loess Plateau.

161 Based on the soil data, the distribution of earth-rock mountain in study area is drawn as Fig.
162 4(b). There were 83 soil types in the study area and 15 of them are composed of earth and rock
163 involving 70 hydrological response units (HRUs) (Table 1). At the same time, these 15 soil types
164 distribute mainly in the Qinling Mountain and Liupan Mountain (Fig. 2). And the earth-rock
165 mountain area accounts for 24% of study area.

166 **2.4 Meteorological and hydrological data**

167 The meteorological data were obtained from the China Meteorological Data Sharing Service
168 System (<http://www.eservice.gov.cn/metdata/page/index.html>) and some local rainfall stations.
169 The data include atmospheric pressure, mean (minimum and maximum) temperature, vapor
170 pressure, relative humidity, rainfall, wind speed, wind direction, sunshine time. Figure 5 (a) shows
171 the distribution of meteorological stations and the annual average precipitation over Wei River
172 basin, which was calculated using kriging interpolation method of ArcGIS 9.3 based on annual
173 average precipitation of 34 meteorological stations. Then the time series of annual average
174 precipitation for the three regions of the study area were calculated respectively using elevation
175 bands method of ArcSWAT (Soil and Water Assessment Tool) 2009.93.7b, which can account for
176 orographic effects on precipitation (Neitsch et al., 2011). SWAT allows the subbasin to be split

177 into a maximum of ten elevation bands. Precipitation is calculated for each elevation band as a
178 function of the respective lapse rate and the difference between the gage elevation and the average
179 elevation specified for the band. Once the precipitation values have been calculated for each
180 elevation band in the subbasin, new average subbasin precipitation value is calculated based on
181 the fraction of subbasin area within the elevation band (Neitsch et al., 2011).

182 And the daily streamflow data of three hydrological stations were obtained from Ecological
183 Environment Database of Loess Plateau (<http://www.loess.csdb.cn/pdmp/index.action>) and the
184 Hydrological Year books of China. Figure 6 shows the time-series of average precipitation, annual
185 streamflow and runoff coefficients for the 3 regions of study area. And the runoff coefficients were
186 0.13, 0.35 and 0.17 on average for region 1, 2 and 3 over the past 50 years (1960-2009).

187 90-meter resolution digital elevation model (DEM) (Fig. 5 (b)) was used to define the
188 topography and delineate the watershed boundary. It was obtained from the Computer Network
189 Information Center, Chinese Academy of Sciences (<http://srtm.datamirror.csdb.cn/>), based on the
190 Shuttle Radar Topography Mission (SRTM) version 4.1.

191 **3. Methods**

192 **3.1 The SWAT model**

193 The SWAT model is developed by the USDA Agricultural Research Service (ARS). It is a
194 physically based and distributed hydrological model. The SWAT model has been widely applied to
195 understand the impact of land management practices on water, sediment and agricultural yields
196 over large complex watersheds with varying soils, land use and management conditions over long
197 periods (Arnold et al., 2009). It is forced with meteorological data, and input with soil properties,
198 topography, land use, and land management practices in the catchment. The physical processes

199 associated with hydrological cycle and sediment movement etc. are directly modeled by SWAT
 200 using these input data (Arnold et al., 2009). In addition, the ArcSWAT extension (ArcSWAT
 201 2009.93.7b version) is used as the graphical user interface for the SWAT model (Gassman et al.,
 202 2007; Arnold et al., 1998).

203 **3.2 The SWAT Model setup**

204 The SWAT model setup includes four steps: watershed delineation, hydrological response
 205 unit (HRU) analyst, input database building and modification and model operation. Based on
 206 research of the Wei River (Shao, 2013b; Wang, 2013), the extraction threshold, which is the
 207 minimum drainage area required to form the origin of a stream, of subbasin area was 80 km². The
 208 Linjiacun, Weijiabu and Xianyang hydrological stations were loaded manually as subbasin outlets
 209 and one whole watershed outlet was defined. The study area was divided into 308 subbasins (Fig.
 210 2). The land area in a subbasin can be further divided into the HRUs, which is the basic computing
 211 element of the SWAT model. In this study, a subbasin was subdivided into only one HRU that was
 212 characterized by dominant land use and soil type. Then the daily meteorological data, including
 213 temperature, relative humidity, sunshine duration, wind speed, rainfall, were input and all data
 214 were written into database building and modification to force the SWAT model.

215 For evaluating the performance in the model calibration and validation, we use the R² and NS
 216 coefficient to evaluate the performance rating of the model (Nash and Sutcliffe, 1970) (Equation
 217 (1) & (2)).

$$218 \quad R^2 = \frac{\left[\sum_{i=1}^n \left(O_i^{obs} - \overline{O_i^{obs}} \right) \left(O_i^{sim} - \overline{O_i^{sim}} \right) \right]^2}{\sum_{i=1}^n \left(O_i^{obs} - \overline{O_i^{obs}} \right)^2 \left(O_i^{sim} - \overline{O_i^{sim}} \right)^2} \quad \text{Eq. (1)}$$

219
$$NS = 1 - \frac{\sum_{i=1}^n (O_i^{obs} - O_i^{sim})^2}{\sum_{i=1}^n (O_i^{obs} - \overline{O_i^{obs}})^2}$$
 Eq. (2)

220 where n is the number of observations, O_i^{obs} is the observed value, O_i^{sim} is the simulated value, and
 221 the overbar means the average of the variable. The R^2 describes the proportion of the variance in
 222 measured data explained by the model and typically 0.5 is considered an acceptable threshold
 223 (Santhi et al., 2001; Van Liew and Garbrecht, 2003). The SWAT model simulation can be judged
 224 as “satisfactory” if the $NS > 0.50$ for a monthly time step simulation and the performance rating of
 225 the SWAT model was very good when the $NS > 0.75$, and the model performed good when the
 226 $NS > 0.65$ (Moriassi et al., 2007).

227 **3.3 Calibration and validation of the SWAT model**

228 We setup the SWAT-CUP procedure for the sensitivity analysis, calibration and validation in
 229 our study (Abbaspour, 2007). The sensitivity analysis is carried out by keeping all parameters
 230 constant to realistic values, while varying each parameter within the range assigned in step one.
 231 The sensitive parameters were calibrated using LH-OAT (Latin-Hypercube-One Factor-At-a-Time)
 232 method of the Sequential Uncertainty Fitting (SUFI2) program (Abbaspour, 2007; Xu et al., 2012).
 233 And the t-stat and p-value were used to evaluate the sensitivity of parameters. The t-stat is the
 234 coefficient of a parameter divided by its standard error and the larger values are more sensitive.
 235 And the p-value determines the significance of the sensitivity and a value close to zero means
 236 more significant. The most sensitive (seven) parameters were selected by the SWAT-CUP module.
 237 Combined with previous research in Wei River, two additional parameters (SOL_K and
 238 GW_DELAY) with the seven parameters were selected in this study (Table 2).

239 The initial value and the range of relevant parameters were derived from simulated rainfall
240 experiments, regional monitoring data and previous research in study area (Wang, 2014; Shao,
241 2013b; Zuo et al., 2015). Vegetation construction changes underlying surface and affects quantity
242 of surface runoff and recharge of both soil and ground water. It has a significant impact on
243 infiltration by providing canopy and litter cover to protect the soil surface from raindrop impacts
244 and producing organic matter which can bind soil particles and increase soil porosity (Le Maitre et
245 al., 1999). These impacts of vegetation on hydrological process are epitomized and reflect by CN
246 and management operation in the SWAT model. the Soil Conservation Service (SCS) curve
247 number equation is the model for computing the amounts of streamflow in SWAT model and its
248 comprehensive parameter is CN which relates to the soil's permeability, land use and antecedent
249 soil water conditions. We have done some research on the impacts of LUCC changes on runoff,
250 infiltration and groundwater under different soil, slope and rainfall intensity in Wei River basin
251 based on simulated rainfall experiments before (Wang, 2014). Based on the experiments, the SCS
252 model and the three-dimensional finite-difference groundwater flow model (MODFLOW) were
253 calibrated and applied also. So values of parameters related to runoff, infiltration and groundwater,
254 such as the initial CN values and recharge rates for different LUCC, specific yield of soil layer etc.
255 were gotten based on experiments and mathematical simulation (Wang, 2014). Meanwhile in the
256 SWAT model, agricultural land and forest have different heat units required for plant maturity and
257 different management operations. The agricultural land includes plant, harvest/ kill and
258 auto-fertilizer operation and the forest only has plant operation. And the management operation of
259 forest involves leaf area index (LAT_INIT), plant biomass (BIO_INIT), age of trees
260 (CURYR_MAT).

261 According to Fig. 1, we could see the revegetation was mainly implemented in the study area
262 after the 1980s. Hence we choose 1960-1969 and 1970-1979 for the model calibration and
263 validation respectively and used the daily streamflow data of the Linjiacun, the Weijiabu and the
264 Xianyang hydrological stations from the upper to middle reaches (the data of 1965 and 1968-1971
265 are missing in the Weijiabu station). The parameters were calibrated for hydrological stations by
266 the order of upstream to midstream using the daily streamflow of 1960-1969. Firstly, the
267 parameters against the streamflow at the Linjiacun control station were calibrated. Secondly,
268 based on the premise of the calibrated parameter values of the Linjiacun station, the parameters
269 were calibrated for the subbasin controlled by the Weijiabu station. In that way, the parameters for
270 the subbasin controlled by the Xianyang station were then calibrated. Then the SWAT model was
271 validated for the three hydrological stations respectively against the streamflow from 1970 to 1979
272 (Fig. 7).

273 **4. Results and discussions**

274 The corresponding statistic results of three hydrological stations showed that the ranges of
275 NS and R^2 were 0.59~0.66 and 0.63~0.68 respectively in the calibration period for a daily time
276 step. And they were 0.57~0.62 and 0.61~0.65 respectively in the validation period. At a monthly
277 time step, the results of the NS and R^2 were 0.82~0.84 and 0.79~0.86 respectively in the
278 calibration period. And they were 0.70~0.76 and 0.74~0.79 respectively in the validation period
279 demonstrating good performance of the model. In addition, the time-series and the patterns of the
280 simulated and observed streamflow during the calibration period and validation period showed
281 similar trends. Our conclusion is that the SWAT model can be used in upper and middle reaches of
282 the Wei River basin.

283 **4.1 Impact of the observed LUCC on streamflow**

284 In order to analyze the impact of the LUCC on streamflow, the land use data of the 1980 and
285 2005 were used in the validated SWAT model. Firstly, the daily streamflow from 1980 to 2009
286 were simulated using observed daily meteorological forcing data and topography, soil data in
287 study area. Secondly, the LUCC data of 1980 was replaced by that of 2005 and their relevant
288 parameters of corresponding land use type were also replaced. We used the LUCC data of 2005
289 but the same meteorological data to simulate the daily streamflow from 1980 to 2009.

290 The change of annual streamflow based on LUCC data of 2005 compared with LUCC data of
291 1980 showed that annual streamflow decreased during 20-year in 30-year ((1980-2009)) and the
292 annual average reduction was 2.0 mm/yr for these 20- year in study area. This is mainly because
293 over different land use types hydrological responds differently even to the same meteorological
294 forcings. For example, rainfall intensity was of great importance influencing to hydrological
295 process of the Wei River, which locates in semi-dry and semi-humid region (Lacombe et al., 2008;
296 Wang, 2014). Results of rainfall numerical experiments showed when the rainfall intensity was
297 smaller or larger, the rainfall would infiltrate into soil or flow away as surface runoff mainly on
298 both grass land and bare slope, while when the rainfall intensity was medium, the rainfall would
299 infiltrate into grass land and flowed away as surface runoff on bare slope (Tobella et al., 2014;
300 Wang, 2014). To reduce influence of meteorological conditions and isolate the impact of the
301 LUCC on streamflow, the 30-year (1980-2009) values of the streamflow for forest and agricultural
302 land were averaged respectively. For period of 1980-2009, we just used their measured and
303 long-term daily meteorological data in the study area to drive the validated model for the designed
304 hydrological experiments. Figure 8 shows the changes of streamflow, surface runoff, soil flow and

305 baseflow between agricultural land and forest. The surface runoff, soil flow and baseflow all
306 decreased for agricultural land, while the soil flow and baseflow of forest increased. Overall, the
307 streamflow decreased in agricultural land and increased in forest area. When the LUCC data are
308 classified and re classified in SWAT model, the tree types are summarized as Range-Brush
309 (RNGB), Forest-Mixed (FRST) and Forest-Deciduous (FRSD). Different types have different
310 hydrological responses for their leaf, roots and so on. We also analyzed the streamflow generation
311 of the main types of forest (RNGB, FRST and FRSD) in study area further. Results showed that
312 the streamflow yield of FRST and FRSD were about 1.20 and 1.60 times of that of RNGB
313 respectively.

314 **4.2 Hydrological experiments on the impact of conversion of** 315 **agricultural land to forests on streamflow**

316 Because the LUCC data involves various land use interconversions, of particular interest here
317 the impact of conversion of cropland to forest on streamflow cannot be distinguished. Starting
318 from the LUCC data of 1980 as (S1) the present land use, we design other four scenarios (Table 3)
319 that (S2) 10%, (S3) 20%, (S4) 40% and (S5) 100% of the agricultural land was converted into
320 Forest-Mixed (FRST) respectively.

321 Based on the five scenarios, the SWAT simulations were conducted to analyze the effect of
322 forest constructions on the streamflow in upper and middle reaches of the Wei River basin. Firstly,
323 the converted agricultural land area was controlled proportionately as same as the variational area
324 ratios of set scenarios in 3 regions divided by Linjiacun, Weijiabu and Xianyang hydrological
325 stations (Fig. 6(a)). Secondly, lands with the same soil type and similar slope were the priorities
326 choosing as the converted land. Thirdly, the converted lands were distributed evenly as much as

327 possible in 3 regions. The simulation period was from 1980 to 2009.

328 We present the distribution of average streamflow change under S2 ~ S5 scenarios compared
329 with S1 scenario in Fig. 9. It shows that the streamflow generally increased when the land use
330 converted from agricultural land into forest in the upstream. And Fig. 10 shows the change rate of
331 streamflow at the Linjiacun, Weijiabu and Xianyang stations correspondingly for its annual
332 average and annual average over non-flood season (Jan - Jun and Nov - Dec). Compared with the
333 S1 scenario, the annual average streamflow increases in the non-flood season were 12.70 %,
334 11.21 % and 9.11% for the Linjiacun, Weijiabu and Xianyang stations with per 10% area of
335 agricultural land converted into forest. Interestingly the average annual streamflow increases were
336 11.61%, 21.63%, 42.51% and 109.25% for S2, S3, S4 and S5 scenario respectively (Fig. 10 (b)),
337 which almost consistently suggested about 1.1% per 1% change of the agricultural land. The
338 results are important in that one can expect that for a 0.8% increase in the forest in the observed
339 LUCC would lead to less than 1% change in the streamflow, which is negligible.

340 To be more comparable, Fig. 11 shows the distribution of the annual runoff coefficients with
341 the scenario changed from S1 to S5. The spatial variability in mean runoff coefficient was large,
342 which ranges from 0.03 to 0.68 and increased with more forest converted from agricultural land.
343 The annual average runoff coefficient of study area increased from 0.21 to 0.37 with forest area
344 increasing from S1 to S5 (Fig. 12). On average, the runoff coefficient increased about 0.014 (i.e.,
345 1.4% of rainfall transformed into streamflow) with per 10% area of agricultural land converted
346 into forest.

347 The landscape of the Wei River is mixed with the Loess Plateau and earth-rock mountain
348 landscapes, which induce different mechanisms of transforming rainfall into streamflow. The

349 earth-rock mountain area accounts for 24.03% of study area (Fig. 4 (b)). In earth-rock mountain
350 area, vegetation grows on much thinner soil layer over the earth-rock mountain. And the soil has
351 high infiltration ability for high stone fragment content. The thin soil is apt to be saturated and
352 produce more soil flow on relatively impermeable rock, hence the streamflow in wooded areas is
353 larger than that in adjacent woodless areas favoring streamflow production (Liu and Zhong, 1978).
354 On the contrary, in Loess Plateau there is existing a drying layer of soil underneath forestland in
355 great water deficit. When the agricultural land converted into forest, the precipitation, intercepted
356 by vegetation, infiltrated into soil and supplied the drying layer of soil, vegetation growth, etc.
357 Together with much thicker soil layer on the Loess Plateau, it usually prevents gravitational
358 infiltration into groundwater and reduces streamflow recharge (Li, 2001; Tian, 2010). The
359 observed results of precipitation and streamflow in study area also showed the runoff coefficients
360 had obviously positive correlation with rates of earth-rock mountain area. The regional annual
361 averages of runoff coefficient were 0.13, 0.17 and 0.35 for Fig. 6 (b), (d) and (c), while the rates of
362 earth-rock mountain area were opposite correspondingly (Fig. 4 (b)). The complication is that the
363 overall effect of forest on the streamflow is in fact a balance between earth-rock mountain positive
364 and Loess Plateau negative effects on the streamflow.

365 Combined with the spatial distribution of precipitation (Fig. 5 (a)), we can see earth-rock
366 mountain landscapes are mainly distributed in regions with more rainfall. To be precise, the whole
367 earth-rock mountain area located where rainfall was greater than 500 mm/yr and over 62% of the
368 study area where the annual rainfall is greater than 600 mm was in earth-rock mountain.
369 Meanwhile, the river network over the earth-rock mountain is denser and most of tributaries in the
370 earth-rock mountain are close to the main stream of the Wei River. Moreover, there distribute a lot

371 of developed gravel riverbed in piedmont, sandy soil along the river and its groundwater level is
372 shallow, which facilitate rainfall infiltration and recharging streamflow. Therefore although the
373 area of earth-rock mountain accounts for 24% of the study area, its distribution areas are
374 concentrated in the main regions of streamflow yield of the study area. Therefore the overall result
375 of balance among all factors was that the forest constructions have positive effect on streamflow.

376 **4.3 Impact of conversion of agricultural land to forests on baseflow**

377 In Fig. 10 (a), one important point is that the average increase in the non-flood season was
378 about 1.41 times larger than the annual increase of the streamflow. To understand that, Fig. 13
379 shows distribution of the baseflow index, i.e., the ratio between baseflow and streamflow, under
380 S1~S5 scenarios. We can see that the baseflow index also increased with land use converted from
381 agricultural land into forest, which means that groundwater contribution to the streamflow
382 increased with the overall increase of forest area. Putting the pictures together, Fig. 14 shows the
383 changes of the streamflow and the baseflow under the S2~S5 scenarios minus those results under
384 the S1 scenario in the non-flood season. The average increases of streamflow and baseflow were
385 1.14 and 0.98 mm/yr with per 1% increase of forest area respectively. For the non-flood season,
386 they were 0.60 and 0.53 mm/yr. The increase of the streamflow contributed by the increased
387 baseflow was about 88.33% in the non-flood season. So the increasing streamflow was mainly
388 contributed by groundwater with increasing of forest area overall.

389 **5. Conclusion**

390 The large scale implementation of Grain for Green project in China is expected to alter
391 hydrological cycle, in particular on the Loess Plateau, within the Yellow River Basin. The
392 scientific question is how large the impact of the LUCC on the streamflow and its components in

393 that area. We choose the Wei River as the study area, in that it has been widely implemented
394 revegetation constructions since the 1980s. Of particular interest here, the landscape of the upper
395 and middle reaches of the Wei River basin is mixed with the Loess Plateau and rocky mountain,
396 which would induce different mechanisms of generating surface runoff, soil flow, base flow and
397 therefore streamflow.

398 To investigate it, we setup the SWAT model for the upper and middle reaches of the Wei
399 River basin with the inputs of long term observed meteorological forcing data, hydrological data,
400 and observed land use data. We use daily and monthly streamflow of the Linjiacun, Weijiabu and
401 Xianyang hydrological stations from upper to middle reaches during 1960-1969 and 1970-1979
402 respectively for the model calibration and model validation. The results showed that the
403 Nash-Sutcliffe (NS) coefficients and the coefficients of determination (R^2) were > 0.57 and 0.61
404 for daily streamflow and 0.70 and 0.74 for monthly streamflow respectively demonstrating that
405 the SWAT model can be used in this study.

406 We analyse the impact of the LUCC on streamflow based on the observed LUCC data of
407 1980 and 2005. The daily streamflow from 1980 to 2009 were simulated using observed daily
408 meteorological data with the two different land use data. The results showed that two-thirds of
409 annual streamflow decreased and the change of streamflow was different among different land use.
410 On the overall average, the 30-year averages of the streamflow decreased in agricultural land but
411 increased in forest. To interpret the overall result, we design five scenarios in this study including
412 (S1) the present land use of 1980 and the scenarios where agricultural land was converted into
413 forest by 10% (S2), 20% (S3), 40% (S4) and 100% (S5) respectively. Based on the five scenarios,
414 we use the calibrated and validated SWAT model to analyze the effect of forest constructions on

415 the streamflow in detail. The results confirm that annual streamflow consistently increased with
416 more forest converted from the agricultural land. Interestingly, the rate is almost consistently 7.41
417 mm/yr per 10% increase of forest converted from the agricultural land. Based on detailed analysis
418 of each component of streamflow, we found it was most attributed by the baseflow. The overall
419 effect of LUCC on the streamflow in the Wei River basin, the largest branch of the Yellow River is
420 the result of the balance between Loess Plateau negative and earth-rock mountain positive effects.
421 Our results here are not only of great importance in understanding the impact of LUCC on
422 streamflow for a catchment with much complicated and mixed landscape, but also of significance
423 for water resources managing practice.

424 **Data availability**

425 The data used in this manuscript were obtained from reliable public data repositories. The
426 LUCC and soil data were obtained from the National Science & Technology Infrastructure of
427 China, the National Earth System Science Data Sharing Infrastructure (<http://www.geodata.cn>).
428 The DEM data were obtained from the Computer Network Information Center, the Chinese
429 Academy of Sciences (<http://srtm.datamirror.csdb.cn/>). The meteorological data were obtained
430 from the China Meteorological Data Sharing Service System
431 (<http://www.escience.gov.cn/metdata/page/index.html>). The daily streamflow data were from the
432 Ecological Environment Database of Loess Plateau (<http://www.loess.csdb.cn/pdmp/index.action>)
433 and the Hydrological Year books of China.

434 **Acknowledgment**

435 This research was supported by the National Key Research and Development Program of
436 China (2016YFA0602402), an Open Research Fund of State Key Laboratory of Desert and Oasis

437 Ecology, Xinjiang, Institute of Ecology and Geography, Chinese Academy of Sciences,
438 CPSF-CAS Joint Foundation for Excellent Postdoctoral Fellows, National Key Research and
439 Development Program of China (2016YFC0401401), the Chinese Academy of Sciences (CAS)
440 Pioneer Hundred Talents Program, the International Science and Technology Cooperation
441 Program of China (2014DFA71910). We thank the Editor and reviewers for valuable comments
442 that improved the manuscript.

443 **References**

- 444 Abbaspour, K. C.: User manual for SWAT-CUP, SWAT calibration and uncertainty analysis programs,
445 Swiss Federal Institute of Aquatic Science and Technology, Eawag, Duebendorf, Switzerland, 2007.
- 446 Arnold, J., Srinivasan, R., Neitsch, S., George, C., Abbaspour, K., Gassman, P., Hao, F. H., Van
447 Griensven, A., Gosain, A., and Debels, P.: Soil and Water Assessment Tool (SWAT): Global
448 Applications, WASWC, 2009.
- 449 Arnold, J. G., Srinivasan, R., Muttiah, R. S., and Williams, J. R.: Large area hydrologic modeling and
450 assessment part I: Model development1, *JAWRA Journal of the American Water Resources Association*,
451 34, 73-89, 1998.
- 452 Beck, H. E., Bruijnzeel, L. A., Dijk, A. I. J. M. V., and Mcvicar, T. R.: The impact of forest regeneration
453 on streamflow in 12 meso-scale humid tropical catchments, *Hydrology & Earth System Sciences*
454 *Discussions*, 10, 3045-3102, 2013.
- 455 Bosch, J. M., and Hewlett, J.: A review of catchment experiments to determine the effect of vegetation
456 changes on water yield and evapotranspiration, *Journal of hydrology*, 55, 3-23, 1982.
- 457 Bradshaw, C., Sodhi, N., Peh, K., and Brook, B.: Global evidence that deforestation amplifies flood
458 risk and severity in the developing world, *Global Change Biology*, 13, 2379–2395, 2007.
- 459 Chen, Y., Wang, K., Lin, Y., Shi, W., Song, Y., and He, X.: Balancing green and grain trade, *Nature*
460 *Geoscience*, 8, 739-741, 2015.
- 461 Deng, L., Liu, G. B., and Shangguan, Z. P.: Land-use conversion and changing soil carbon stocks in
462 China's 'Grain-for-Green' Program: a synthesis, *Global Change Biology*, 20, 3544–3556, 2013.
- 463 Dijk, A. I. J. M. V., Noordwijk, M. V., Calder, I. R., Bruijnzeel, S. L. A., Schellekens, J., and Chappell,
464 N. A.: Forest–flood relation still tenuous – comment on ‘Global evidence that deforestation amplifies
465 flood risk and severity in the developing world’ by C. J. A. Bradshaw, N.S. Sodi, K. S.-H. Peh and B.W.
466 Brook, *Global Change Biology*, 15, 110-115, 2009.
- 467 Farley, K. A., Jobbágy, E. G., and Jackson, R. B.: Effects of afforestation on water yield: a global
468 synthesis with implications for policy, *Global Change Biology*, 11, 1565-1576, 2005.
- 469 Foley, J. A., Ruth, D., Asner, G. P., Carol, B., Gordon, B., Carpenter, S. R., F Stuart, C., Coe, M. T.,
470 Daily, G. C., and Gibbs, H. K.: Global consequences of land use, *Science*, 309, 570-574, 2005.
- 471 Hibbert, A. R.: Forest Treatment Effects on Water Yield, Pennsylvania Univ University, 527-543, 2001.
- 472 Huang, B. W.: Several issues of the impact of forest on environment, *China Water Resouces*, 4, 29-32,
473 1982.

474 Huang, Z. G., Ouyang, Z. Y., Li, F. R., Zheng, H., and Wang, X.: Progress in the Effects of Forest
475 Ecosystem on Runoff Based on Forest Catchments, *World Forestry Research*, 22, 36-41, 2009.

476 D., Janeau, J. L., Soulléuth, B., Robain, H., Taccon, A., Sengphaathith, P., Mouche, E.,
477 Sengtaeuanghoung, O., Tran Duc, T., Valentin, C.: Contradictory hydrological impacts of afforestation
478 in the humid tropics evidenced by long-term field monitoring and simulation modelling, *Hydrology &
479 Earth System Sciences*, 20, 2691-2704, 2016.

480 Lacombe, G., Cappelaere, B., Leduc C.: Hydrological impact of water and soil conservation works in
481 the Merguellil catchment of central Tunisia, *Journal of Hydrology*, 359, 210-224, 2008.

482 Lacombe, G., Ribolzi, O., de Rouw, A., Pierret, A., Latschak, K., Silvera, N., Pham Dinh, R., Orange,
483 Lørup, J. K., Refsgaard, J. C., and Mazvimavi, D.: Assessing the effect of land use change on
484 catchment runoff by combined use of statistical tests and hydrological modelling: case studies from
485 Zimbabwe, *Journal of Hydrology*, 205, 147-163, 1998.

486 Le Maitre, D. C., Scott, D. F., and Colvin, C.: Review of information on interactions between
487 vegetation and groundwater, *Water Research Commission*, 25, 137-152, 1999. Li, W. H., He, Y. T., and
488 Yang, L. Y.: A summary and perspective of forest vegetation impacts on water yield, *Journal of Natural
489 Resources*, 16, 398-406, 2001.

490 Li, Y. S.: Effects of forest on water circle on the Loess Plateau, *Journal of Natural Resources*, 16,
491 427-432, 2001.

492 Lin, Q. C., and Li, H. E.: Influence and guarantee on ecological basic flow of Weihe River from
493 Baojixia water diversion, *Journal of Arid Land Resources and Environment*, 24, 114-119, 2010.

494 Liu, C. M., and Zhong, J. X.: The influence of forest cover upon annual runoff in the Loess Plateau of
495 China, *Acta Geographica Sinica*, 33, 112-126, 1978.

496 Liu, Y., and Hu, A. Y.: Changes of Precipitation Characters Along Weihe Basin in 50 Years and Its
497 Influence on Water Resources, *Journal of Arid Land Resources & Environment*, 20, 85-87, 2006.

498 Lorup, J. K., and Hansen, E.: Effect of land use on the streamflow in the southwestern highlands of
499 Tanzania, *International Symposium on Sustainability of Water Resources Under Increasing Uncertainty,
500 at the 5th Scientific Assembly of IAHS, RABAT, MOROCCO*, 1997.

501 Mango, L., Melesse, A., McClain, M., Gann, D., and Setegn, S.: Land use and climate change impacts
502 on the hydrology of the upper Mara River Basin, Kenya: results of a modeling study to support better
503 resource management, *Hydrology and Earth System Sciences*, 15, 2245-2258, 2011.

504 Moriassi, D. N., Arnold, J. G., Van Liew, M. W., Bingner, R. L., Harmel, R. D., and Veith, T. L.: Model
505 evaluation guidelines for systematic quantification of accuracy in watershed simulations, *Trans. Asabe*,
506 50, 885-900, 2007.

507 Nash, J., and Sutcliffe, J. V.: River flow forecasting through conceptual models part I—A discussion of
508 principles, *Journal of hydrology*, 10, 282-290, 1970.

509 Neitsch, S. L., Arnold, J. G., Kiniry, J. R., Williams, J. R.: *Soil and Water Assessment Tool (SWAT)
510 Theoretical Documentation: Version 2000*, Texas Water Resources Institute Technical Report No. 406,
511 2011.

512 Ogden, F. L., Crouch, T. D., Stallard, R. F., and Hall, J. S.: Effect of land cover and use on dry season
513 river runoff, runoff efficiency, and peak storm runoff in the seasonal tropics of Central Panama, *Water
514 Resources Research*, 49, 8443-8462, 2013.

515 Price, K.: Effects of watershed topography, soils, land use, and climate on baseflow hydrology in
516 humid regions: A review, *Progress in physical geography*, 35, 465-492, 2011.

517 Shao, H., Baffaut, C., Gao, J. E., Nelson, N. O., Janssen, K. A., Pierzynski, G. M., Barnes, P. L.:

518 Development and application of algorithms for simulating terraces within SWAT, Transactions of the
519 Asabe, 56, 1715-1730, 2013a.

520 Shao, H.: Simulation of Soil and Water Loss Variation toward Terrace Practice in the Weihe River
521 Basin, Doctor, Northwest A & F University, Yangling Shaanx, 2013b.

522 Smith, R., and Scott, D.: The effects of afforestation on low flows in various regions of South Africa,
523 Water S. A., 18, 185-194, 1992.

524 Sriwongsitanon, N., and Taesombat, W.: Effects of land cover on runoff coefficient, Journal of
525 Hydrology, 410, 226-238, 2011.

526 Tian, J. L.: Environmental effects of Loess Plateau Ecological Construction, China Meteorological
527 Press, Beijing, 2010.

528 Tobella, A. B., Reese, H., Almaw, A., Bayala, J., Malmer, A., Laudon, H., and Ilstedt, U.: The effect of
529 trees on preferential flow and soil infiltrability in an agroforestry parkland in semiarid Burkina Faso,
530 Water Resources Research, 50, 3342-3354, 2014.

531 Van Liew, M. W., and Garbrecht, J.: Hydrologic simulation of the Little Washita River experimental
532 watershed using SWAT, Journal of the American Water Resources Association, 39, 413-426, 2003.

533 VanShaar, J. R., Haddeland, I., and Lettenmaier, D. P.: Effects of land - cover changes on the
534 hydrological response of interior Columbia River basin forested catchments, Hydrological Processes,
535 16, 2499-2520, 2002.

536 Wagner, P. D., Kumar, S., and Schneider, K.: An assessment of land use change impacts on the water
537 resources of the Mula and Mutha Rivers catchment upstream of Pune, India, Hydrology & Earth
538 System Sciences, 10, 1943-1985, 2013.

539 Wang, F.: Study of runoff and value of ecosystem based on landuse change in Weihe River basin,
540 Master, Northwest A & F University, Yangling Shaanxi, 2013.

541 Wang, H.: The Effects of Typical Measures of Soil and Water Conservation on Ecological Basic Flow
542 Recharged from Groundwater, Doctor, University of Chinese Academy of Sciences, Beijing, China,
543 2014.

544 Wang, L. X.: Effect of construction and protective of vegetation on protection and utilization of water
545 resources, Xiangshan Conference, Beijing, 2000.

546 Wang, Y. H., Yu, P. T., Feger, K. H., Wei, X. H., Sun, G., Bonell, M., Xiong, W., Zhang, S. L., and Xu,
547 L. H.: Annual runoff and evapotranspiration of forestlands and non - forestlands in selected basins of
548 the Loess Plateau of China, Ecohydrology, 4, 277-287, 2011.

549 Woodward, C., Shulmeister, J., Larsen, J., Jacobsen, G. E., and Zawadzki, A.: Landscape hydrology.
550 The hydrological legacy of deforestation on global wetlands, Science, 346, 844-847, 2014.

551 Wang, Y., Shao, M., Shao, H.: A preliminary investigation of the dynamic characteristics of dried soil
552 layers on the Loess Plateau of China, Journal of Hydrology, 381, 9-17, 2010 a.

553 Wang, Y., Shao, M., Liu, Z.: Large-scale spatial variability of dried soil layers and related factors across
554 the entire Loess Plateau of China, Geoderma, 159, 99-108, 2010 b. Xu, Y. D., Fu, B. J., and He, C. S.:
555 Assessing the hydrological effect of the check dams in the Loess Plateau, China by model simulations,
556 Hydrology & Earth System Sciences Discussions, 9, 13491-13517, 2012.

557 Yan, Y., Tian, J., Fan, M. S., Zhang, F. S., Li, X. L., Christie, P., Chen, H. Q., Lee, J., Kuzyakov, Y., and
558 Six, J.: Soil organic carbon and total nitrogen in intensively managed arable soils, Agriculture,
559 ecosystems & environment, 150, 102-110, 2012.

560 Zuo, D., Xu, Z., Zhao, J., Abbaspour, K. C., and Yang, H.: Response of runoff to climate change in the
561 wei river basin, china. Hydrological Sciences Journal/journal Des Sciences Hydrologiques, 60, 1-15,

562 2015.Zhang, H., and Hiscock, K.: Modelling the impact of forest cover on groundwater resources: A
563 case study of the Sherwood Sandstone aquifer in the East Midlands, UK, Journal of hydrology, 392,
564 136-149, 2010.
565 Zhang, T. Z.: Based on hydrological characteristics of Donggou and Xigou catchment in Yongding
566 River to analyze the hydrological function of forest vegetation, Resources Science, 90-98, 1984.

567 **Figure Captions:**

568 **Fig. 1** The development of soil and water conservation measures in the main stream basin of Wei River
569 over last 50 years.

570 **Fig. 2** The study area: the Wei river basin on the Loess Plateau.

571 **Fig. 3** The observed land use data of the year 1980 and the year 2005 in study area.

572 **Fig. 4** The Soil data and the distribution of earth-rock mountain in study area.

573 **Fig. 5** The spatial distribution of annual average precipitation in Wei River basin over the past 55 years
574 (1956-2010) and the DEM of study area.

575 **Fig. 6** The time-series of precipitation, annual streamflow and runoff coefficients for the regions of
576 study area.

577 **Fig.7** The time-series graphs of calculated vs. observed values during calibration period and
578 verification period for hydrological stations.

579 **Fig. 8** The changes of 30-year (1980-2009) averages of streamflow, surface runoff, soil flow and
580 baseflow between agricultural land and forest.

581 **Fig. 9** The watershed distribution of average streamflow change under S2~S5 scenarios compared with
582 S1 scenario.

583 **Fig. 10** The corresponding proportional change rate of streamflow at Linjiacun, Weijiabu and Xianyang
584 station for annual average and annual average in non-flood season.

585 **Fig. 11** The distribution of annual runoff coefficient with the scenario changed from S1 to S5.

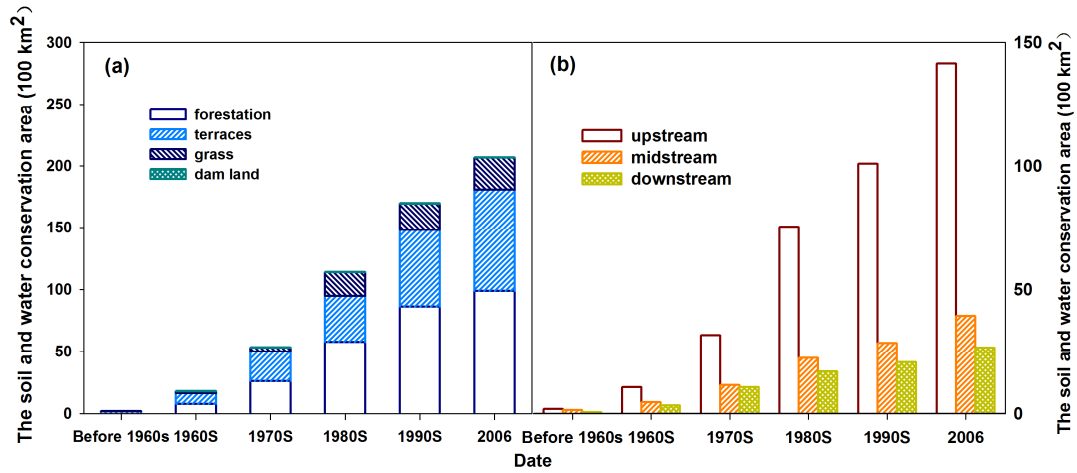
586 **Fig. 12** The annual average runoff coefficient of study area with forest area increasing from S1 to S5.

587 **Fig. 13** The distribution of baseflow index under S1~S5 scenarios.

588 **Fig. 14** The corresponding change of streamflow and baseflow under S2~S5 scenarios compared with

589 S1 for annual average of year and non-flood season.

590



591

592 **Fig. 1** The development of soil and water conservation measures in the main stream basin of Wei River

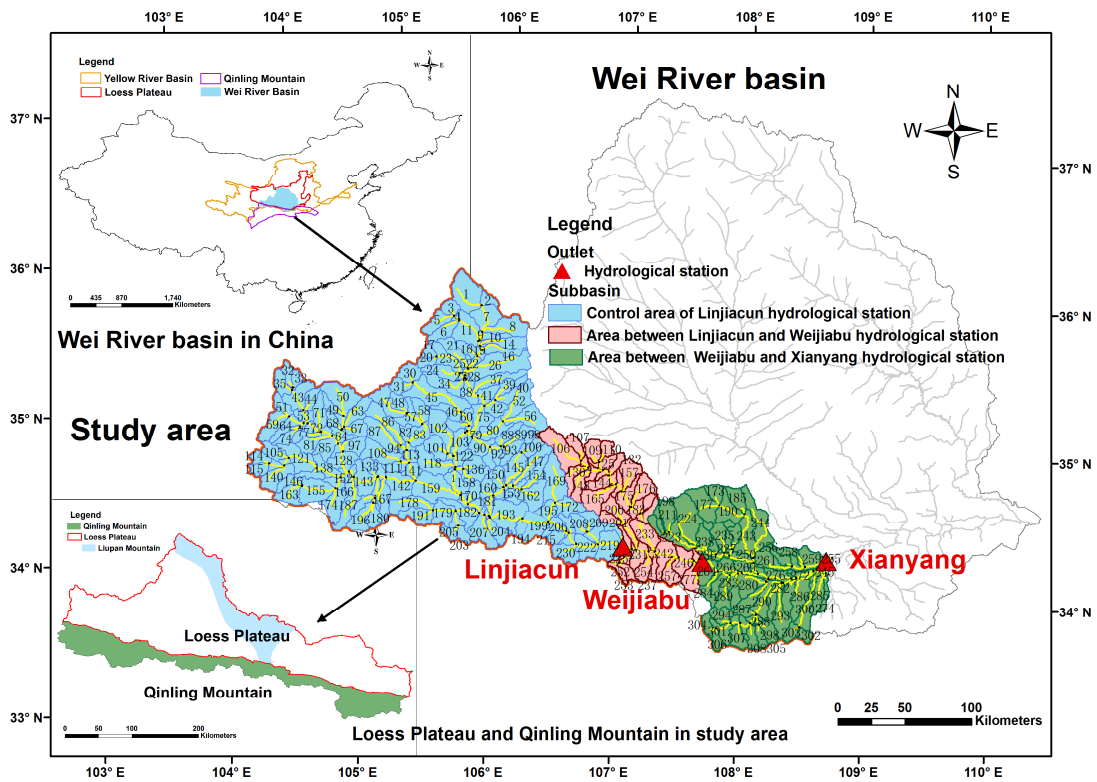
593

over last 50 years

594 Figure 1 (a) is the area developing of forestation, terraces, grass and dam land separately. Figure

595 1(b) is the sum area of the forestation, terraces, grass and dam land in upstream, midstream

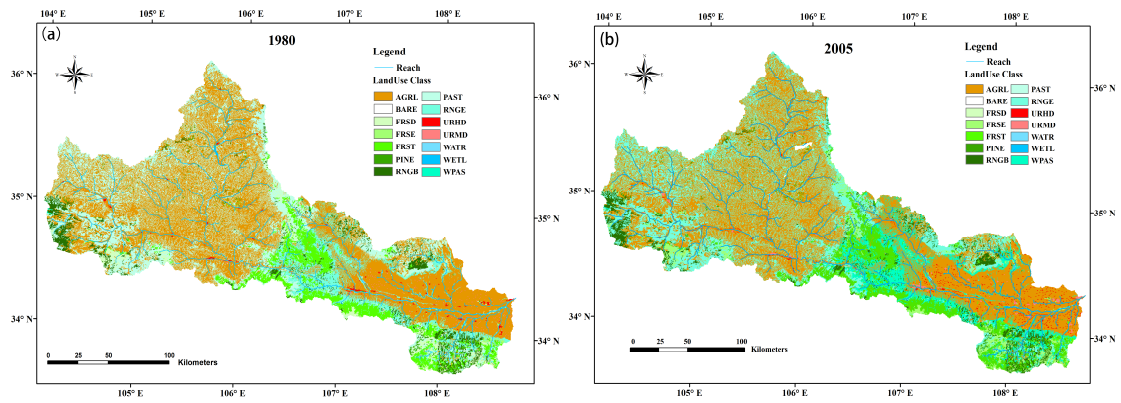
596 and downstream.



597

598

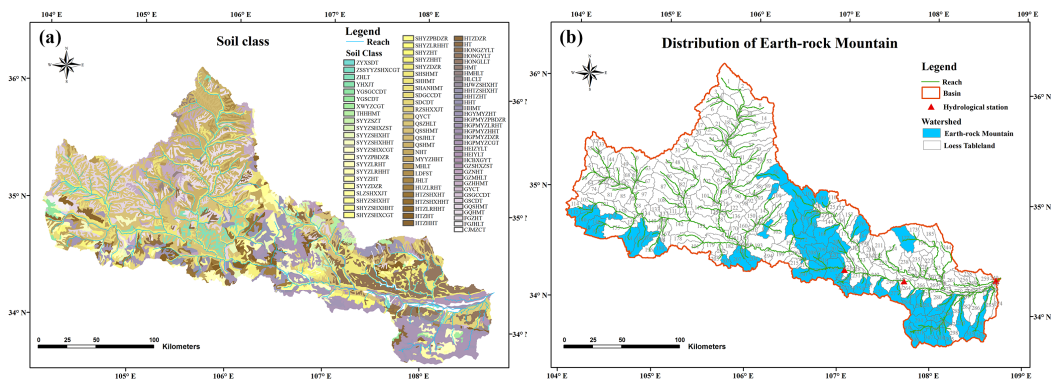
Fig. 2 The study area: the Wei river basin on the Loess Plateau.



599

600

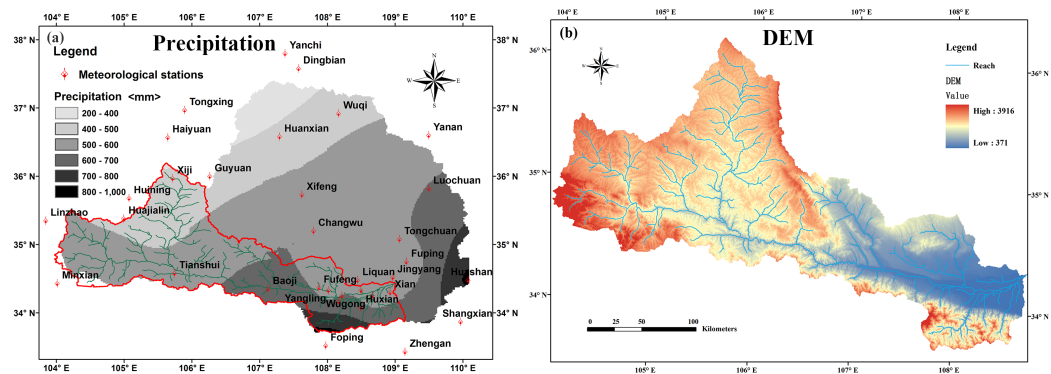
Fig. 3 The observed land use data of the year 1980 and the year 2005 in study area



601

602

Fig. 4 The Soil data and the distribution of earth-rock mountain in study area



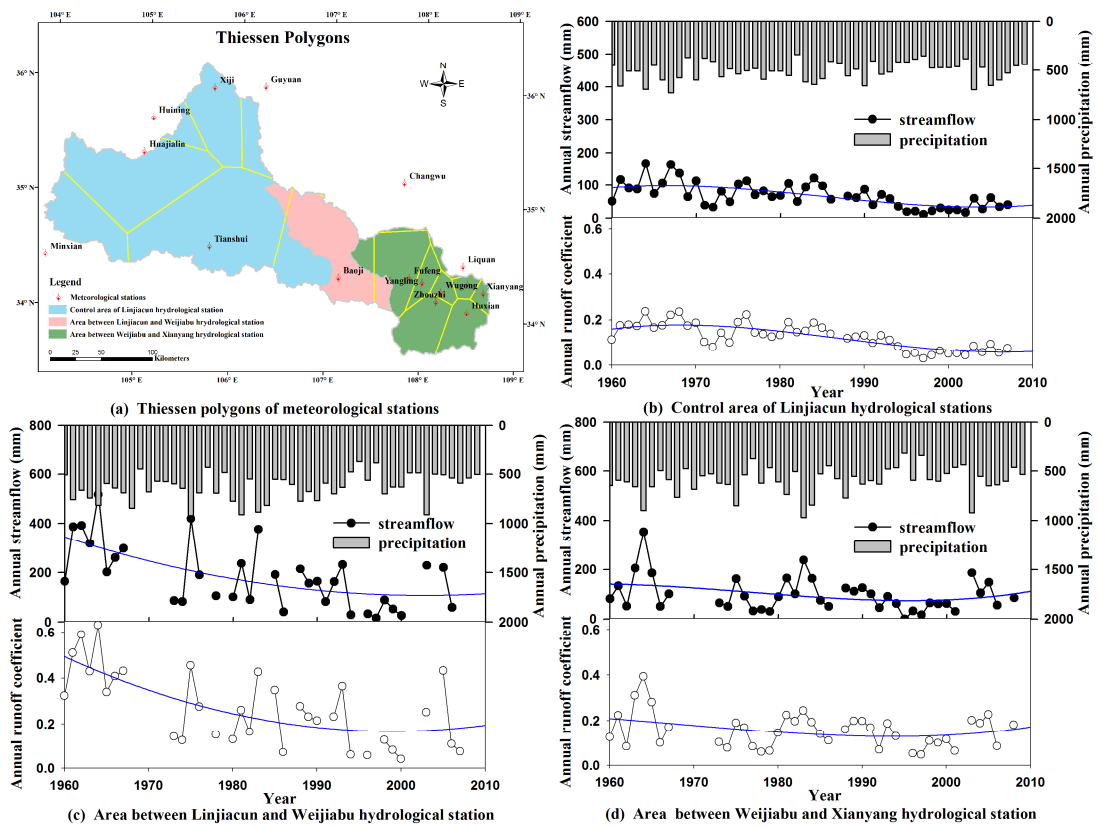
603

604

Fig. 5 The spatial distribution of annual average precipitation in Wei River basin over the past 55 years

605

(1956-2010) and the DEM study area



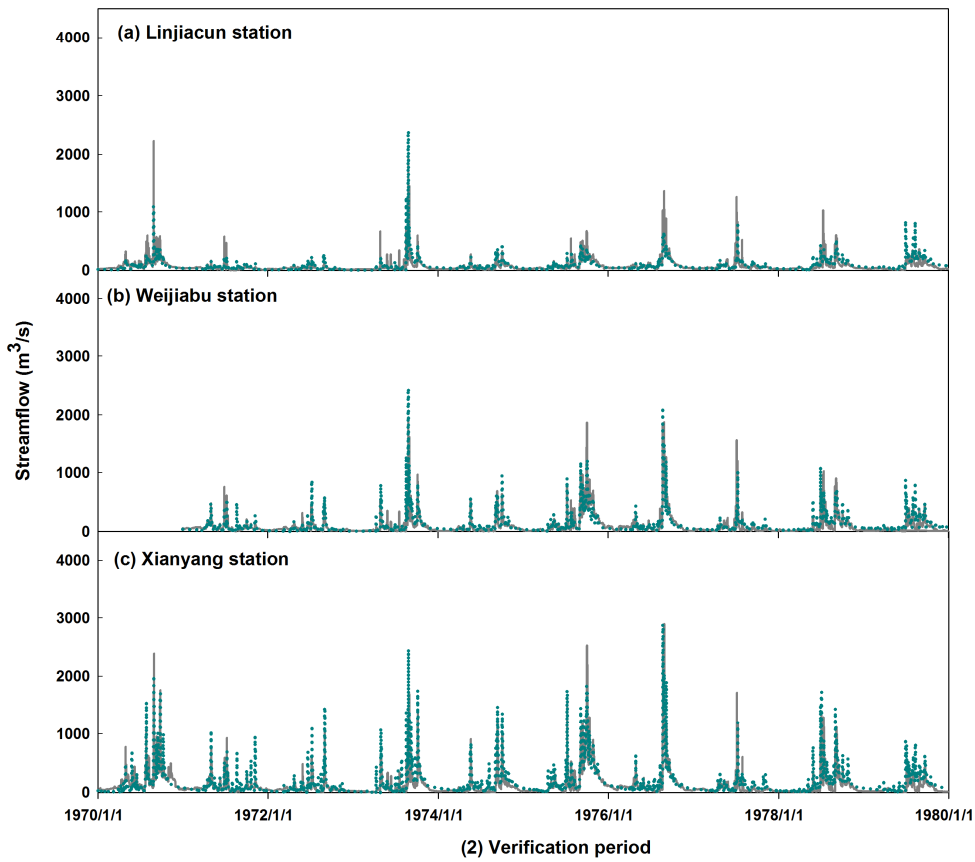
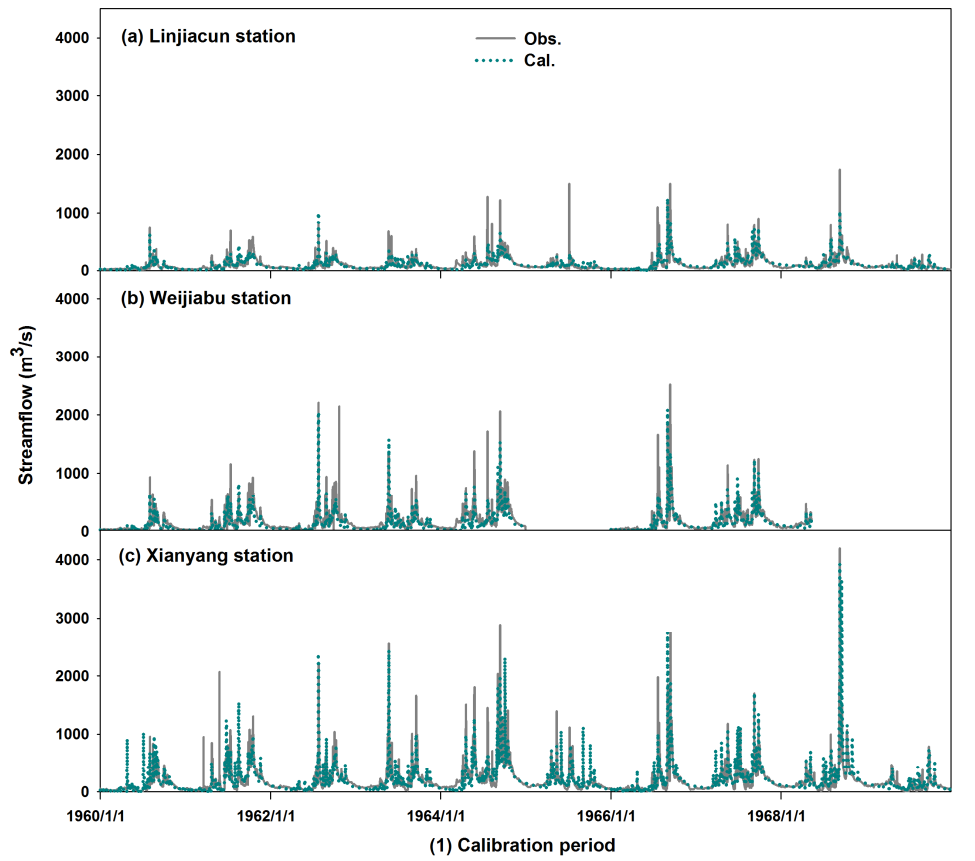
606

607

Fig. 6 The time-series of precipitation, annual streamflow and runoff coefficients for the regions of

608

study area



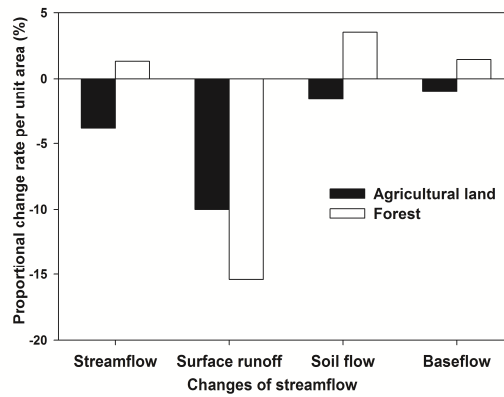
609

610

Fig. 7 The time-series graphs of calculated vs. observed values during calibration period and verification

611

period for hydrological stations



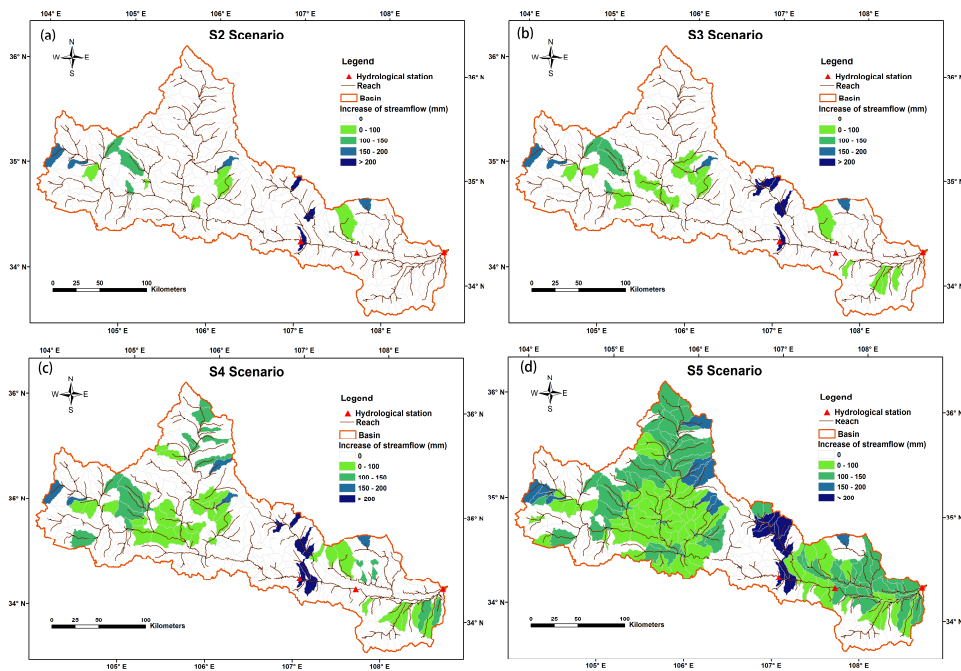
612

613

Fig. 8 The changes of 30-year (1980-2009) averages of streamflow, surface runoff, soil flow and

614

baseflow between agricultural land and forest



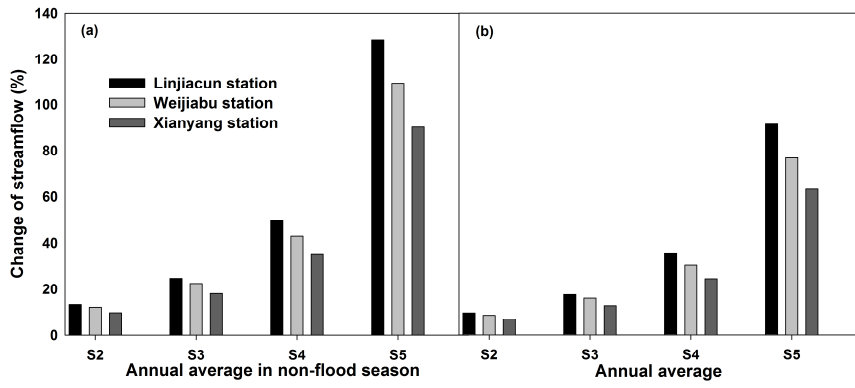
615

616

Fig. 9 The watershed distribution of average streamflow change under S2~S5 scenarios compared with

617

S1 scenario

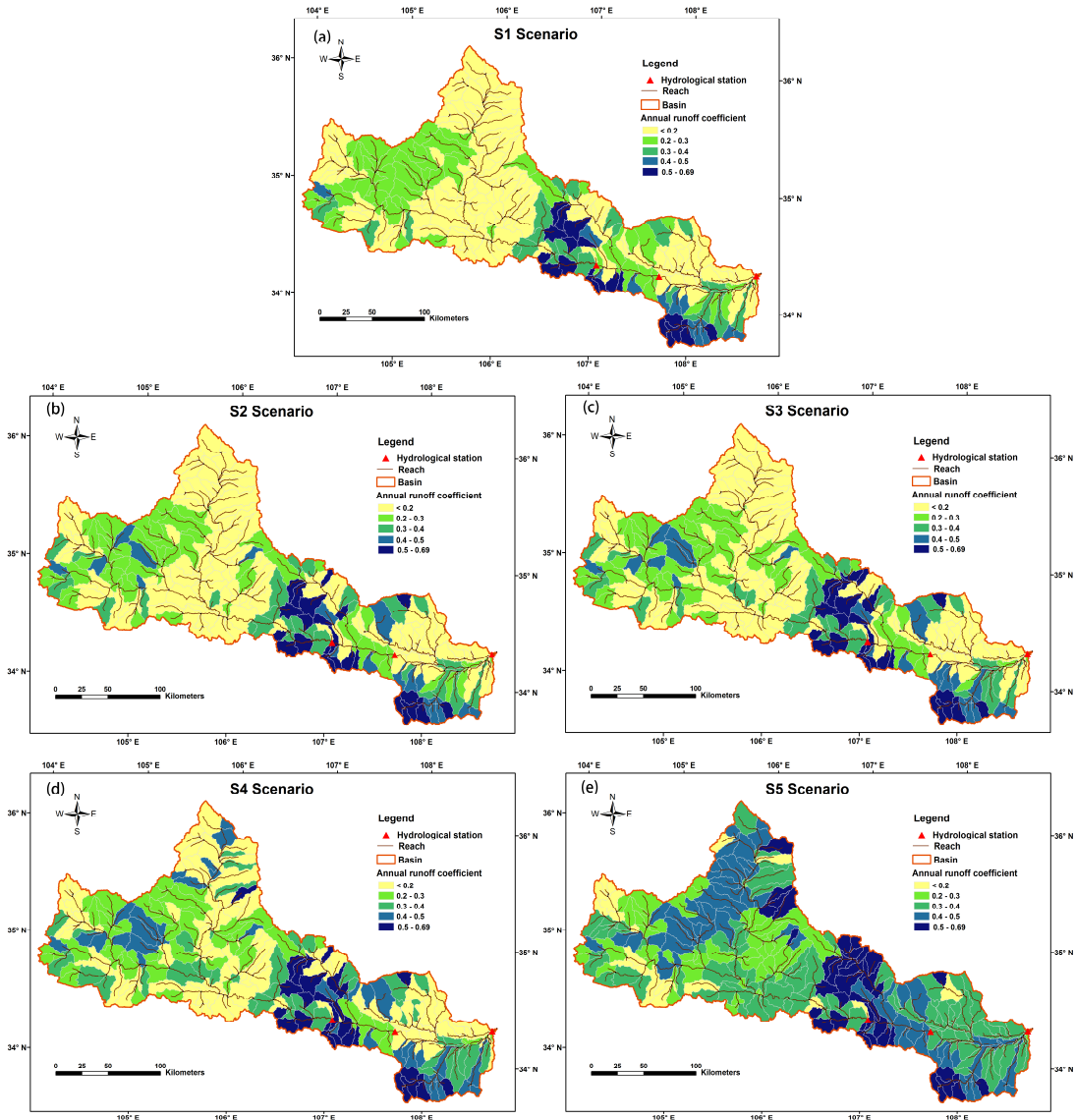


618

619 **Fig.10** The corresponding proportional change rate of streamflow at Linjiacun, Weijiabu and Xianyang

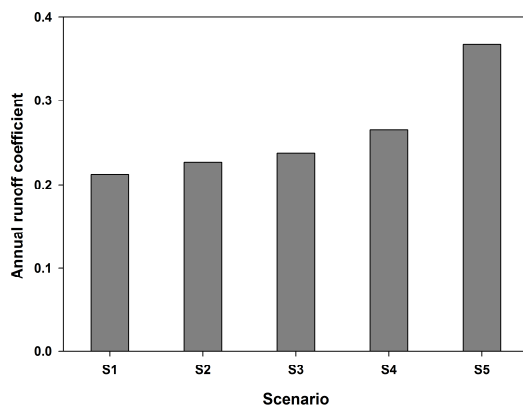
620

station for annual average and annual average in non-flood season



621

622 **Fig. 11** The distribution of annual runoff coefficient with the scenario changed from S1 to S5

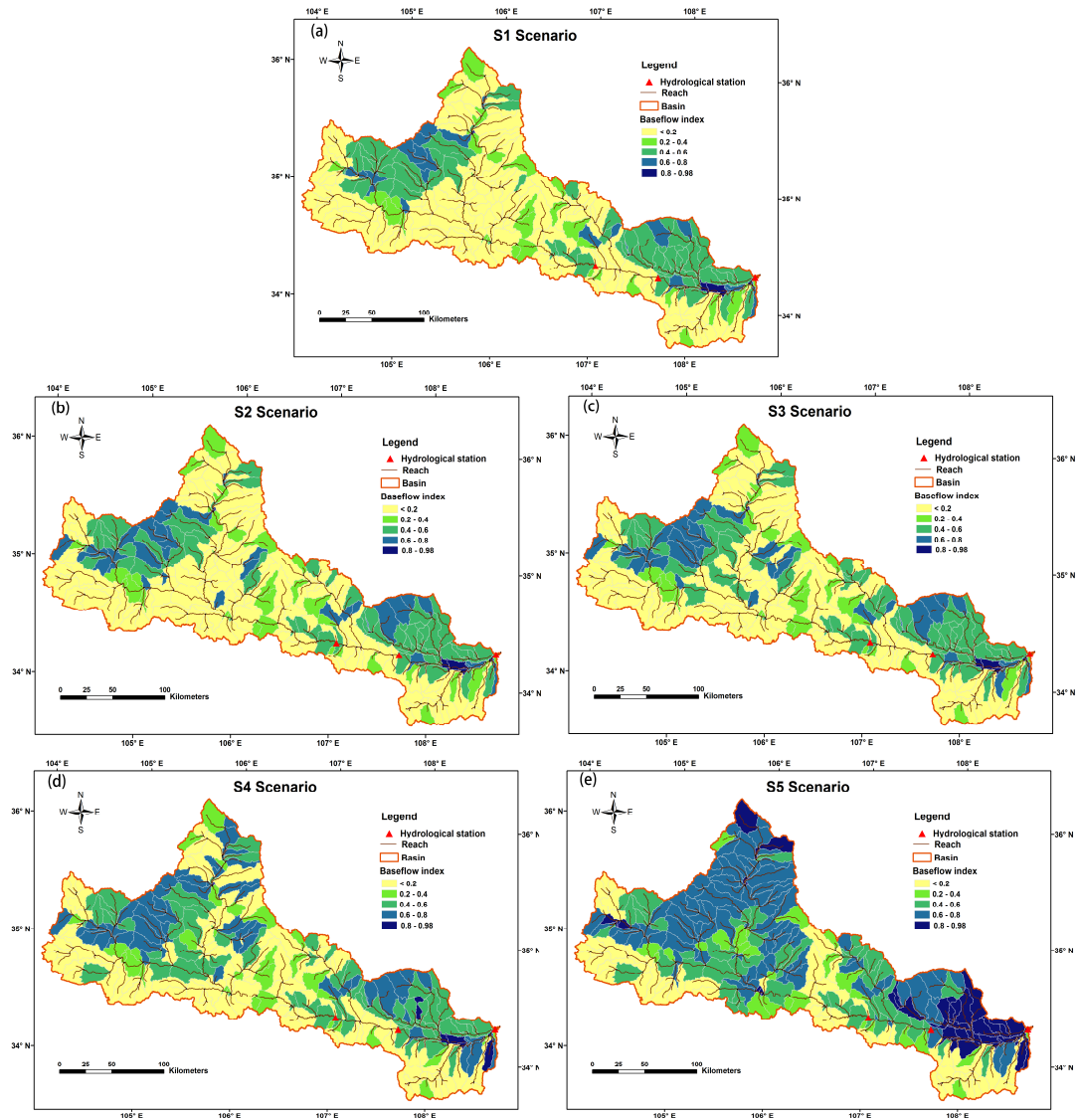


623

624

Fig. 12 The annual average runoff coefficient of study area with forest area increasing from S1 to S5

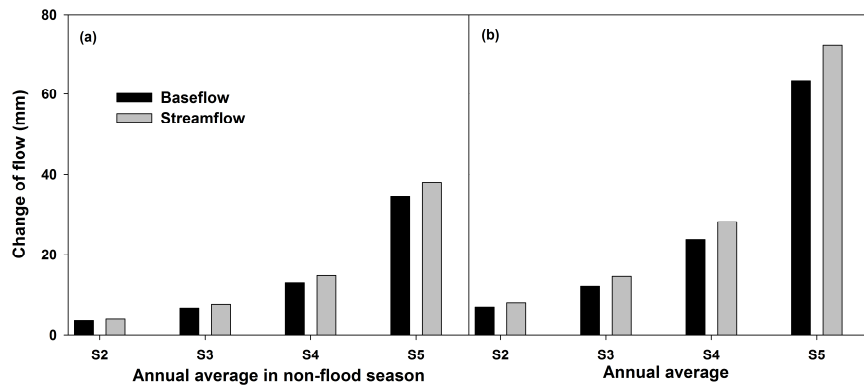
625



626

627

Fig. 13 The distribution of baseflow index under S1~S5 scenarios



628

629 **Fig.14** The corresponding change of streamflow and baseflow under S2~S5 scenarios compared with

630

S1 for annual average of year and non-flood season

631 Tables

632

Table 1 The soil type and its distribution of earth-rock mountain in study area

| No. | Code of Soil type | Physical meaning of the code | HRU | Area (km ²) |
|-----|-------------------|-------------------------------------------|-----------------------------------------------------------------------------------------------|-------------------------|
| 1 | SHYZHT | Limestone Cinnamon soil | 220, 257 | 26316.90 |
| 2 | SHYZSHXHT | Limestone Calcic cinnamon soil | 153 | 11471.22 |
| 3 | SYYZLRHT | Sandstone—shale Luvic cinnamon soil | 166, 203, 207 | 50065.29 |
| 4 | HGPMYZLRHT | Granite—gneiss Luvic cinnamon soil | 174, 180, 187, 201, 204, 221, 277, 283, 287 | 158397.93 |
| 5 | SYYZDZR | Sandstone—shale Light brown earth | 106, 169, 299 | 103955.40 |
| 6 | HGPMYZDZR | Granite—gneiss Light brown earth | 130, 148, 172, 209, 252, 284, 289, 290, 291, 293, 294, 300, 301, 302, 303, 305, 306, 307, 308 | 299737.26 |
| 7 | HGPMYZPBDZR | Granite—gneiss Light brown earth | 253 | 8739.90 |
| 8 | MYYZHHT | Sandstone—shale Grey cinnamon soil | 115, 117, 146, 163 | 51204.96 |
| 9 | SYYZSHXHHT | Sandstone—shale Calcic grey cinnamon soil | 99, 129 | 19392.21 |
| 10 | SHYZSHXHHT | Limestone Calcic Grey cinnamon soil | 56 | 33885.54 |
| 11 | SYYZSHXZST | Sandstone—shale Purple soil | 109, 176, 177, 184, 200 | 106159.41 |
| 12 | HGPMYZCGT | Granit—gneiss Rhogosol | 165, 230, 237, 254, 271, 292, 295, 296, 297, 304 | 112136.40 |
| 13 | SYYZSHXCGT | Sandstone—shale Rhogosol | 107, 208, 213, 216, 218, 219, 248 | 87612.84 |
| 14 | SHYZSHXCGT | Limestone Rhogosol | 222 | 23375.79 |
| 15 | SYYZLRHHT | Sandstone—shale Luvic grey | 116, 140 | 30320.73 |

| | | | | |
|--|--|---------------|--|--|
| | | cinnamon soil | | |
|--|--|---------------|--|--|

633

634

Table 2 Calibrated values of model parameters

| Parameters | Physical meaning | Calibration range | Calibration result | | |
|------------|--------------------------------------------------------------|----------------------|--------------------|--------------|--------------|
| | | | Linjiac un | Weijia bu | Xianya ng |
| r_CN2 | Initial SCS runoff curve number for moisture condition II | -0.3~0.3 | -0.27 | 0.05 | -0.17 |
| r_SOL_AWC | Available water capacity of soil layer | -0.6~0.6 | 0.01 | -0.01 | -0.01 |
| r_SOL_K | Saturated hydraulic conductivity of soil layer (mm/hr) | -0.5~0.5 | 0.5 | 0.3 | 0.5 |
| r_HRU_SLP | Average slope stepness (m/m) | -0.5~1.5 | 1.5 | 0.41 | 0.52 |
| r_SLSUBBSN | Average slope length (m) | -0.5~1.5 | 1.17 | 0.70 | 1.20 |
| v_ALPHA_BF | Baseflow alpha factor | 0~1.0 | 0.48 | 0.61 | 0.61 |
| v_GW_DELAY | Groundwater delay (days) | 0~500 | 220 | 38 | 62 |
| v_ESCO | Soil evaporation compensation factor | 0~1.0 | 0.65 | 0.90 | 0.80 |
| v_CH_K2 | Effective hydraulic conductivity in main channel alluvium | 0~130 | 5 | 30 | 30 |

635

Notes: v__ means the existing parameter value is to be replaced by the given value; r__ means the existing parameter value is multiplied by (1+ a given value).

636

637

638

Table 3 Scenarios for simulation

| Scenario | Description | Area (km ²) | The average simulated streamflow |
|----------|-------------------|-------------------------|--------------------------------------------------|
| | | | (1980-2009) (10 ⁸ m ³ /yr) |
| S 1 | present situation | 0 | 50.44 |

| | | | |
|-----|---------------------------------|----------|-------|
| S 2 | 10% agricultural land → forest | 2937.63 | 53.92 |
| S 3 | 20% agricultural land → forest | 5875.26 | 56.83 |
| S 4 | 40% agricultural land → forest | 11750.53 | 62.73 |
| S 5 | 100% agricultural land → forest | 29376.32 | 82.28 |

639 Notes: ① Agricultural land refers to the land for crops planting, including cultivated land, newly cultivated soil, fallow field,
640 rotation plot, pasture-crop rotation and land used for agro-fruit, agro-mulberry, agroforestry (The code in model is AGRL). ②
641 Forest refers to the natural forest and plantation, which canopy density is larger than 30%, including timberland, economic forest,
642 protection forest (The code in model is FRST).
643